Mean First-Passage Times of Looping of Polymers with Intrachain Reactive Monomers: Lattice Monte Carlo Simulations

Ting Cui,[†] Jiandong Ding,*,[†] and Jeff Z. Y. Chen*,[†,‡]

Key Laboratory of Molecular Engineering of Polymers of Chinese Ministry of Education, Department of Macromolecular Science, Fudan University, Shanghai 200433, China, and Department of Physics, University of Waterloo, Waterloo, Ontario, Canada N2L 3G1

ABSTRACT: Using Monte Carlo simulations, we study the diffusion-controlled dynamics of a polymer chain, which leads to the intrachain reaction of two reactive monomers. On the basis of the bond fluctuation lattice model, we computed the mean first-passage time and examined its scaling behavior as a function of the chain length and location of the reactive monomers, for five different types of polymer architectures. While the simulation results confirmed previous theoretical predictions for the free chain case, our measurements of the mean first-passage time also yielded new insights into the looping dynamics of end-grafted chains.

I. Introduction

Polymer looping is one of the basic dynamic processes that commonly occur in many synthetic and biological macromolecules. The simplest case involves two reactive monomers separated by a long distance along the polymer contour path. During looping, these two monomers approach each other within a physical distance comparable to the force range of the attraction between them and start the next stage of a physical or chemical process that directly involves the interaction between the two interacting monomers. The conformational fluctuations of the entire chain, not the interaction between the interacting monomers (for a short-ranged interaction), control the dynamic process of looping that can be characterized by the basic chain parameters such as the chain length, the excluded-volume between two monomers, the location, and the force range of the two interacting monomers.

Much attention has been placed to the simple case of looping between two terminal ends of a basic Gaussian chain. Wilemski and Fixman[1,2] considered the diffusion-controlled intrachain reaction on the basis of a theoretical treatment of the dynamics of polymers.[3] They invoked a decoupling approximation whose validity has been reexamined very recently.[4] Because of the mathematical challenge in the theoretical treatment of the problem, a typical theoretical approach contains various types of approximations.[5–13] For the mean first-passage time, the characteristic time that measures the looping dynamics followed by an irreversible reaction of the two reactive monomers, the scaling behaviors have just been clearly confirmed by computer simulation results[14] of an ideal single chain. A renormalization-group treatment that deals with the looping dynamics of two reacting terminal ends, with the inclusion of an excluded-volume interaction, has also been considered.[15,16] The early- and long-time scales of cyclization of a Gaussian chain have been investigated with Langevin dynamics simulations by Yeung and Friedman.[17,18]

Equally important is the looping dynamics and kinetics of a polymer chain where two reactive monomers are located at any place along the polymer chain. For reversible cyclizations, the dependence of the reaction rate on the position of the reactive monomers and the chain length has recently been examined by Sung et al.[19] with a generalized Wilemski−Fixman treatment, by Ortiz-Repiso et al.[20,21] with Brownian dynamics simulations, and by Sheng et al.[22] with off-lattice Monte Carlo simulations. For diffusion-controlled, irreversible reactions between two reactive monomers, Friedman and O'Shaughnessy have calculated the early- and late-time reaction rates and considered a number of limiting cases where scaling behavior can be written.[23]

Computer simulations avoid potential pitfalls of making approximations in theoretical treatment. A properly constructed model together with adequately sampled statistics would give definitive measurements of physical quantities of interests. Indeed, to study the diffusion-controlled looping, both Brownian dynamics simulations[17,24−26] and Monte Carlo simulations[10,14,27] have been carried out for various models of polymers. Most of these computer simulations, including the work presented in this paper, are limited to the ideal case in the free-draining limit where no hydrodynamic interaction was incorporated in the model.

In this paper, we focus on the comparison of the scaling behavior of the mean first-passage times in five different types of looping scenarios (see Figure 1) by lattice Monte Carlo simulations. All monomers in the model are taken to be identical, with the exception of the grafted monomer in the wall-grafted cases where the grafted monomer is fixed in space. The conformational fluctuations have been simulated by the implementation of the lattice Monte Carlo method (section II). The assumption here is that the Monte Carlo dynamics, represented by an appropriate local move scheme, effectively describe the Brownian dynamics of a real chain.[28,29] The computational results for the mean first-passage times of the five scenarios are discussed in section III.

II. Simulation Method

In a lattice representation, a polymer is described by monomers, each occupying a lattice cell measured $2l \times 2l \times 2l$ on a cubic lattice in three dimensions, as schematically shown in Figure 2. During a Monte Carlo move, an attempt is made to move a monomer to a neighboring site according to the
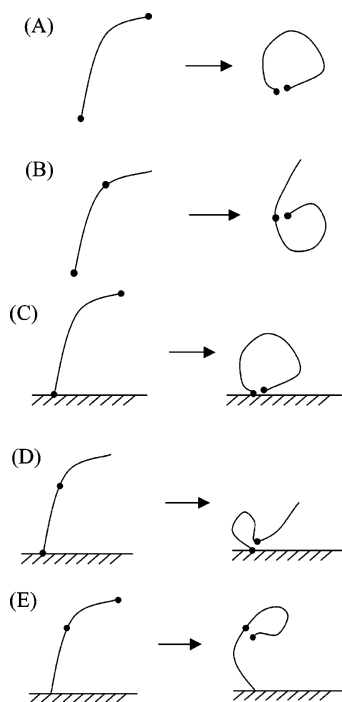
CDV

Figure 1. Schematic representations of loop formation of five different types in chain architecture: looping that leads to the first contact of (A) the terminal ends of a free polymer chain, (B) one terminal end and an interior monomer of a free polymer chain, (C) the terminal ends of a wall-grafted chain, (D) the grafted terminal end and an interior monomer of a wall-grafted chain, and (E) the free terminal end and an interior monomer of a wall-grafted polymer chain. The reactive monomers have been represented by dark circles. In (C), (D), and (E), the wall was treated as a structureless hard surface.
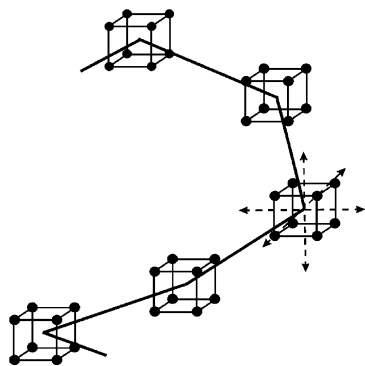

Figure 2. Example of a segment of a lattice polymer used in the current work, as implemented in the bond-fluctuation model. A monomer is represented by a unit cell of the volume $(2l)^3$ and is allowed to move into neighboring sites, subject to the bond-length and excluded-volume restrictions.

prescription of the bond fluctuation model.[30,31] For a polymer consisting of N monomers, N such attempts constitute a Monte Carlo step (MCS), which is considered to be the basic time unit in this article. Statistically each monomer has a chance to move once, during one MCS. The bond fluctuation model is an efficient computer simulation tool for studying polymer dynamics, and essential physical features such as excluded-volume interaction and disallowance of bond crossing are effectively embedded in the model.[30,31] We have followed exactly the same simulation procedure for a three-dimensional system that was originally suggested by Deutsch and Binder.[31] As schematically illustrated in Figure 2, each monomer is allowed to move into one of the nearest-neighbor, unoccupied site groups in a three-dimensional cubic lattice—an underlying reference structure. The
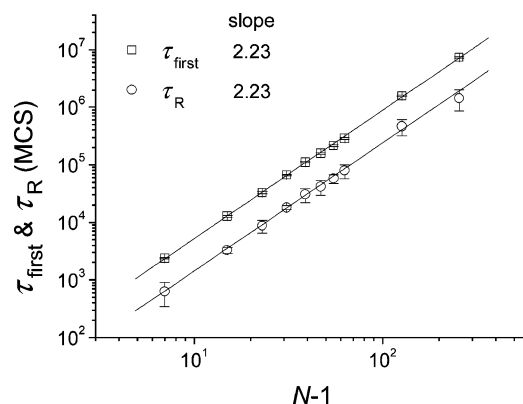

Figure 3. Mean first-passage time (squares), τ_{first}, for a free chain with two reactive terminal ends and the relaxation time (circles), τ_R, of the end-to-end distance vector, as a function of chain length $N - 1$. The error bars of τ_{first} and τ_R are based on the statistics collected from 10^3 and 10^2 independently simulated dynamic events, respectively. The slopes of the double-logarithmic data plots are 2.23 ± 0.02 and 2.23 ± 0.11 for τ_{first} and τ_R, respectively.

bond length between adjacent monomers is allowed to fluctuate within a predetermined range of $2l$ to $\sqrt{10}l$ in three dimensions.[31] From the implementation of the bond-fluctuation model, the average bond length is approximately $b = 2.732l$.

To tailor the simulation procedure for studying the mean first-passage time, for each looping event we prepared an initial configuration after adequate equilibrating time. In the case of a free polymer chain, to computationally generate the modeled chain, we first place a monomer in the center of the coordinate system and then sequentially place other monomers, each separated from the previous one by a distance of $2l$, in a random direction. Then, this preliminary configuration is used as the starting point for a sufficiently long equilibration period of simulation, consisting of ~10 times the relaxation time. For chain length $N = 8$, 16, 24, 32, 40, 48, 56, 64, 128, and 256 examined below, this implies that an initial equilibration period consisting of 5, 20, 50, 100, 150, 250, 300, 400, 1600, and 6400 kMCS has been used.

In each looping event, we began the measurement ($t = 0$) after the chain reached an equilibrated conformation and recorded the first-passage time ($t = t_{first}$) once the distance between two interacting monomers became equal to or smaller than the specified distance. The looping event was then considered complete, and a new initial configuration was prepared.

The Monte Carlo simulations for the looping dynamics of grafted chains proceeded in a similar way as described above. We have further considered the following physical conditions: (1) the grafted terminal is fixed in space; (2) a simulated attempt would be considered to fail if it led a monomer into the wall region; (3) approximately 8 times more Monte Carlo steps were used in the initial equilibrium period, in comparison with those used for the free-chain cases.

For the given force range or a capture radius $2l$ with a fixed polymer chain length N, a total number of M ($M \geq 10^3$) looping events have been simulated. The mean first-passage time presented below, τ_{first}, was taken as the algebraic average of all observed values for t_{first}.

III. Results and Discussion

A. Free Chain with Two Reactive Ends. The mean first-passage time τ_{first} as a function of bond number $N - 1$ is shown in Figure 3 in a double-logarithmic plot. The plot confirms a

CDV

power-law behavior

$$\tau_{\text{first}} \propto (N - 1)^q \tag{1}$$

where $q = 2.23$, from a fitting of the data points in the figure.

Leaving the system of a self-avoiding chain for a moment, for a simple Gaussian chain we know from previous theoretical studies that the mean first-passage time might fall into one of the two scaling regimes:[10] the Rouse regime[1,2,5] and the Szabo−Schulten−Schulten regime.[6,10,13] For the current work, the system is likely to display a scaling behavior similar to that of the Rouse dynamics.[14] In the Rouse regime for large N, the scaling behavior of the mean first-passage time is expected to follow a Rouse behavior

$$\tau_{\text{Rouse}} \propto (N - 1)^{1+2\nu} \tag{2}$$

where ν is the scaling exponent for the root-mean-square end-to-end distance as a function of $N - 1$. For a Gaussian chain, $\nu = 1/2$; hence $q = 2$. Returning to the present system where the excluded-volume interaction is explicitly considered at the athermal state, $\nu \approx 0.59$,[32] we would anticipate that $q \approx 2.18$, assuming that the mean first-passage time is in the Rouse regime. Our numerical results agree with this value within the numerical uncertainty.

For comparison, we can directly determine the kinetic relaxation time of the end-to-end vector of the current model in an equilibrium state. To this end, we have performed a separate set of equilibrium Monte Carlo simulations. The autocorrelation function of the end-to-end distance vector, $\mathbf{R}(t) \equiv \mathbf{r}_N(t) - \mathbf{r}_1(t)$, has been monitored in 100 independent simulated trajectories. We computed the ensemble average

$$f(t) \equiv \langle \mathbf{R}(t) \cdot \mathbf{R}(0) \rangle \tag{3}$$

on the basis of these independent simulations.[33] The numerical value of the relaxation time, τ_R, was then determined from the definition

$$\tau_R(N) = \int_0^\infty t f(t)\, dt / \int_0^\infty f(t)\, dt \tag{4}$$

The relaxation time has been plotted as filled circles in Figure 3, where we clearly see an excellent agreement between the simulation data and the expected relaxation time as scaling exponents are concerned.

B. Free Chain with a Terminal End Reacting with an Interior Monomer. Most theoretical attention has been paid to the simple case of loop formation that is associated with two reactive terminal ends of a polymer. Loop formation that facilitates the contact of a terminal end and an interior monomer has been paid less attention. The latter, however, is highly relevant to many biological looping processes involving the binding of interior monomers between two, or sometimes even more than two, monomers or residues. Sheng et al. have recently performed Monte Carlo simulations to study the characteristic time associated with thermally reversible binding of two interior monomers of an excluded chain and theoretically analyzed this system using an entropy-loss treatment.[22] It is desirable to directly observe the first-passage time, a characteristic time associated with an irreversible binding process (typical of a diffusion-limited process starting from a random conformation), for the current system by computational simulations.

In this section, we consider the mean first-passage time of loop formation between a terminal end and an internal monomer, as schematically shown in Figure 1B. In this case, the distance
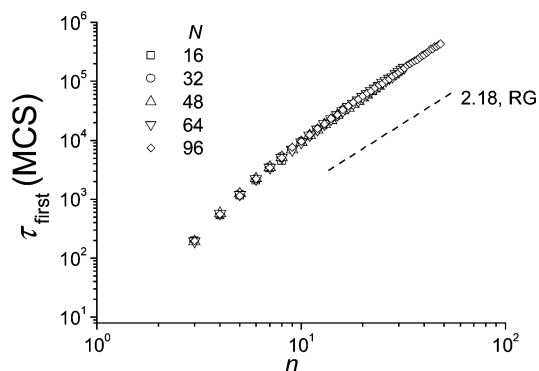

Figure 4. Double-logarithmic plots of the mean first passage time τ_{first} vs n ($\leq 0.5N$) for reaction between a terminal end and an interior monomer that are separated by a distance $n - 1$ along the contour of a self-avoiding polymer with chain length N. In the large n regime our data approach the scaling law in eq 5. The marked scale exponent is from a renormalization group (RG) analysis.[23]

between the two nonbonded monomers along the polymer chain, $n - 1$ ($3 \leq n \leq N$), is another parameter that needs to be taken into consideration.

For a given N, the mean first-passage time, $\tau_{\text{first}}(n,N)$, is a function of both n and N. In the small n/N regime ($n/N < 0.5$), the simulation results for five chain lengths are shown in Figure 4, where the first passage time is mainly controlled by the parameter n and has almost no visible dependence on N; this can be compared with a similar conclusion made by Ortiz-Repiso et al.,[20] who have conducted Brownian dynamic simulations of the same system. Figure 4 is a double-logarithmic plot where the data points approach a straight line at relatively large n. On the basis of this we can write

$$\tau_{\text{first}}(n,N) \propto n^p \quad (1 \ll n \ll N) \tag{5}$$

Note that p is not an independent exponent. Consider the ratio

$$\frac{\tau_{\text{first}}(n,N)}{\tau_{\text{first}}(N,N)} \propto \left(\frac{n}{N}\right)^q n^{(p-q)} \tag{6}$$

for long polymers where we expect a scaling behavior; this should be dependent on n/N only, and hence $p = q = 2.18$ (see also a renormalization group analysis by Friedman and O'Shaughnessy[23]). Our data can be seen to converge to this asymptotic behavior. In contrast, Ortiz-Repiso and Rey[21] have reported $p = 2.41$ on the basis of their Brownian dynamics simulations of a free-draining self-avoiding chain; this larger p is probably due to the fact that they have considered relatively small n regime in their data analysis. Our data in Figure 4 also show a larger slope in the small n regime, which is not well represented by the scaling behavior in eq 5.

Our data demonstrate that eq 5 is only valid for the $1 \ll n \ll N$ regime. When n is close to N, this single power law, however, breaks down. The simulation results for $N = 16, 32, 48, 64,$ and 96 display a maximum near $n_{\max}/N \approx 0.9$ for each given N. Figure 5A shows that these results overlay on top of each other in a plot using scaled axes. As can be inferred from the figure, we see that within the simulation accuracy the data points collapse into a universal scaling behavior

$$\tau_{\text{first}}(n,N) = \tau_{\text{first}}(n_{\max},N)\, g(n/N) \tag{7}$$

where the function $g(x)$ contains a maximum near $x_{\max} \approx 0.9$. The existence of this maximum has not been observed previously in either Brownian dynamics simulations of the same

CDV

system[20,21] or renormalization group analysis[23] by other groups because of the lack of data in the regime near the maximum.

To rule out that the excluded-volume interaction is the cause of the maximum in $g(x)$, we have also computed $\tau_{first}(n,N)$ for a phantom chain where the condition of mutual exclusion between nonneighboring monomers was removed in the computer simulations. Otherwise, the simulations followed exactly the same procedure as those lead to Figure 5A. As can be seen in a scaling plot, Figure 5B, the mean-first passage time also displays a maximum near the same location $n_{max} \approx 0.9N$.

To understand this maximum, in an indirect comparison, we consider the relaxation of the vector $\mathbf{R}_n(t) \equiv \mathbf{r}_n(t) - \mathbf{r}_1(t)$, where $\mathbf{r}_n(t)$ and $\mathbf{r}_1(t)$ are the coordinates of the nth and terminal monomers at time t, respectively. Following the derivation of the normal modes for a Gaussian chain,[3] we can calculate the autocorrelation function for the relaxation of this vector

$$f_n(t) = \langle \mathbf{R}_n(t) \cdot \mathbf{R}_n(0) \rangle \tag{8}$$

Defining a relaxation time

$$\tau_R(n,N) = \int_0^\infty t f_n(t)\, dt / \int_0^\infty f_n(t)\, dt \tag{9}$$

we obtain

$$\frac{\tau_R(n,N)}{\tau_R(N)} \propto \frac{\sum_{p=1}^\infty [\cos(p\pi n/N) - 1]^2 / p^6}{\sum_{p=1}^\infty [\cos(p\pi n/N) - 1]^2 / p^4} \tag{10}$$

where $\tau_R(N)$ is the longest Rouse time of the system. The function on the right-hand side can be computed as the ratio between two summations and displays a weak maximum at $n_{max} \approx 0.87N$, very close to the location of the maxima in Figure 5. The maximal peaks in Figure 5, however, are stronger than that in the relaxation time computation.

Doi has stressed the importance of the short-time modes in the looping dynamics of a polymer.[5] In fact, for polymer looping with two reactive terminal monomers of a reactive radius similar to the bond length, a simple scaling argument shows that all short-time modes would participate.[14] In the current system where one of the reactive monomer is in the interior, we expect that internal dynamic modes, those with short time scales, would become even more important.

There is a lack of theoretical understanding for the first-passage time of reaction between two monomers where at least one of them is in the interior, with and without the presence of the excluded volume. Beyond the difficulty of incorporating the excluded volume in such a calculation, the manifest of the internal dynamic modes would likely complicate the situation even further.

C. Grafted Chain with Two Reactive Terminal Ends. In this section, we consider a grafted polymer that is confined in the positive z space by an impenetrable wall; one terminal end of the polymer is permanently grafted to the hard wall located at $z = l$. Besides these restrictions, the computer simulations for determination of the first-passage time, of looping between two reactive terminal monomers, proceeded exactly the same way as described in section II.

The simulation results are presented in the double-logarithmic plots in Figure 6. Similar to what we have observed in Figure 3, the points of τ_{first} come into a single scaling line, following eq 1, in the limit of $N \gg 1$. Treating all data points equally on
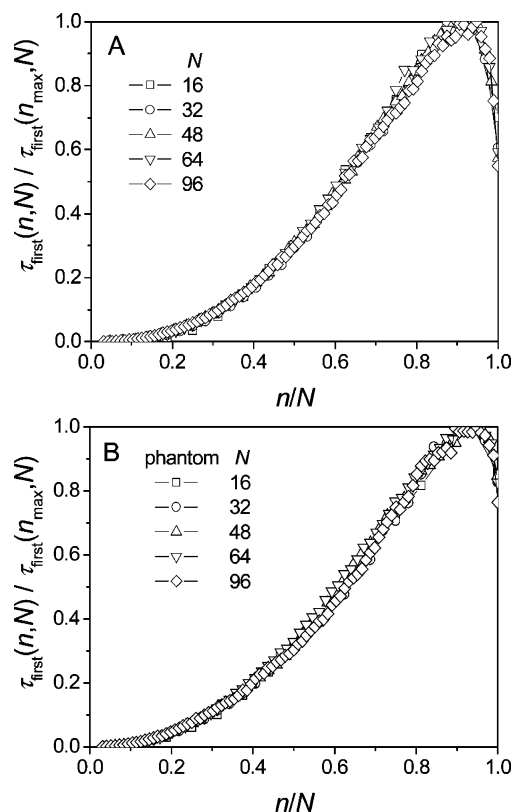
Figure 5. Scaled mean first-passage time for reaction between a terminal end and an interior monomer that are separated by a distance $n - 1$ along the polymer. The mean first-passage time, $\tau_{first}(n,N)$, collected from 2×10^3 independent simulation events, is scaled by the maximum in the $\tau_{first}(n,N)$ curve as a function of n for a given N. The results for both excluded-volume chains (A) and phantom chains (B) are plotted.

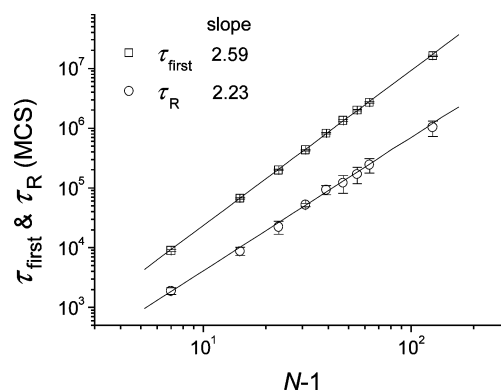**Figure 6.** Mean first-passage time (squares), τ_{first}, of looping between with two reactive terminal ends of a grafted chain and the relaxation time (circles), τ_R, of the end-to-end distance vector. The error bars of τ_{first} and τ_R are based on the statistics collected from 10^3 and 10^2 independently simulated dynamic events, respectively. The slopes of the double-logarithmic data plots are 2.59 ± 0.01 and 2.23 ± 0.08 for τ_{first} and τ_R, respectively.

a double-logarithmic scale, we have obtained a slope, $q = 2.59$, from a least-squares fit. The obtained value of q, however, is greater than the expected $1 + 2\nu$ (see eq 2) of the Rouse time. This difference in the scaling exponents of τ_{first} and τ_R, in the end-grafted case, can be contrasted with those found in section IIIA for a free chain; in the latter case, the scaling exponents are the same. For comparison, we also carried out independent equilibrium simulations, aiming at probing the kinetic relaxation time, τ_R. The relaxation times determined according to eqs 3 and 4 are plotted as filled circles in Figure 5. The slope on the
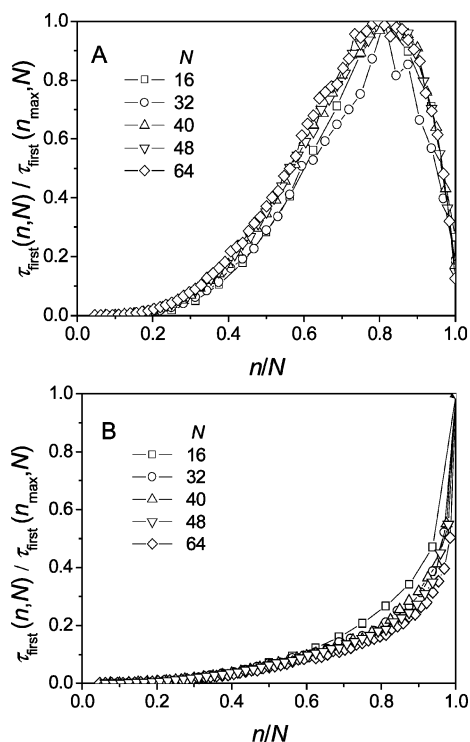
CDV

Figure 7. Scaled mean first-passage time for looping between a reactive terminal end and an interior monomer that are separated by path distance $n - 1$ along a grafted polymer. Different scaling functions have been observed in the cases where the reactive terminal monomer is the grafted monomer (plot A, see Figure 1D) and the reactive terminal monomer is a free monomer (plot B, see Figure 1E). The mean first-passage time, $\tau_{first}(n,N)$, collected from 2×10^3 independent simulation events, is scaled by the maximum in the curve, $\tau_{first}(n_{max},N)$, for a given N.

double-logarithmic plot, 2.23, close to what Kovac pointed out before,[33] confirms that the relaxation time follows the Rouse behavior.

D. Grafted-Chain with a Reactive Terminal End and a Reactive Interior Monomer. In this section, we consider the mean first-passage time, calculated from the Monte Carlo simulations, for the reaction between a terminal end and an interior monomer of a grafted chain. Note that there are two separated cases here: the reactive terminal monomer can be either the grafted monomer (Figure 1D) or the free end (Figure 1E). The simulations were conducted in the same way as in the above section, and the only change is that we monitor the relative distance between the reactive terminal monomer and the reactive monomer, separated by $n - 1$ ($3 \leq n \leq N$) units alone the chain. Various values of chain length N have been taken: $N = 16, 32, 40, 48$, and 64.

The numerical results for $\tau_{first}(n,N)$, scaled by the maximum value of the same function $\tau_{first}(n_{max},N)$ for a given N, are presented as a function of n/N in Figure 7A,B. A direct comparison of mean first-passage times for the three cases is presented in Figure 8. The characteristic features can be drawn on the basis of all of the preceding figures.

First, in both cases where the reactive terminal monomer is the free end or the grafted end, we can see that most data points collapse into a universal curve, except for short chains ($N = 16$ and 32). The two universal curves in Figure 1D,E, however, are distinctively different (Figure 7A,B), reflecting the broken symmetry of the terminal ends of an end-grafted chain.

Second, comparing the systems in parts B and D of Figure 1, we see that the presence of the impenetrable wall in Figure 1D is a hindrance for a monomer to reach the reactive grafted
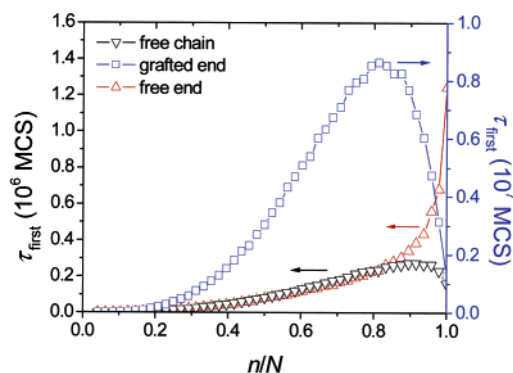

Figure 8. Direct numerical comparison of first passage times for internal looping in the three cases illustrated in Figure 1B (free chain), Figure 1D (grafted end reacting with an interior monomer for a grafted chain), and Figure 1E (free end of a grafted chain reacting with an interior monomer) for chain length $N = 48$. The right vertical axis shows that the values of τ_{first} in the case of "grafted end" are much larger than those in the other two cases.

monomer. As a result, in a direct numerical comparison, for any given n/N, the overall mean first passage time is, according to Figure 8, much greater than that of the system in Figure 1B. For relatively large n/N, the hindrance amplifies the maximum in Figure 5A, which now appears in Figure 7A with a much larger peak (see also Figure 8). A grafted polymer needs to take a unique type of conformation, as illustrated in the second panel of Figure 1D, to make the two reactive monomers approaching each other because of the hard wall. As a result, the maximum peak in Figure 7A is about 1 order of magnitude higher than τ_{first} at $n = N$. For the latter, the effect of the wall is comparatively less important.

Finally, in contrast to Figure 7A, τ_{first} in Figure 7B continuously increases until $n/N \approx 1$. For system in Figure 1E, in small n/N regime, the two reactive monomers are far away from the grafting end and are not influenced by the grafting monomer. As a result, τ_{first} increases as n/N increases, with similar magnitude to τ_{first} in Figure 5A (see also the comparison shown in Figure 8). For large n/N, the interior reactive monomer is close to the grafting end. The presence of the wall causes the reduction of the conformational space for the two reactive monomers to access. This effect becomes more severe as n/N approaches 1. At $n/N = 1$ in Figure 8, τ_{first} of a grafted chain is 1 order of magnitude larger than τ_{first} of a free chain—a property that we can also see in Figure 6 in contrast to Figure 3. The increase of τ_{first} in Figure 7B, in the large n/N regime due to the presence of the wall, is so much more pronounced that the maximum in Figure 5A—presumably due to the internal dynamic modes—is completely overshadowed (as presented in a comparative way in Figure 8). This is the reason for the monotonic increase of τ_{first} in Figure 7B.

IV. Summary

In summary, we have applied a bond fluctuation algorithm to simulate the diffusion-controlled dynamics of reaction between two monomers in a free-draining self-avoiding polymer. We measured and compared the mean first-passage times to characterize the dynamics for five different systems sketched in Figure 1. The simulation results for the free chain are expected and can be accounted for by the current understanding of the problem. However, there is a lack of more quantitative theoretical explanation pertinent for explaining the unique signatures of τ_{first} observed in grafted systems presented in sections IIIC and IIID.

CDV

References and Notes

(1) Wilemski, G.; Fixman, M. *J. Chem. Phys.* **1974**, *60*, 866.
(2) Wilemski, G.; Fixman, M. *J. Chem. Phys.* **1974**, *60*, 878.
(3) Doi, M.; Edwards, S. F. *The Theory of Polymer Dynamics;* Oxford University Press: New York, 1988.
(4) Sokolov, I. M. *Phys. Rev. Lett.* **2003**, *90*, 080601.
(5) Doi, M. *Chem. Phys.* **1975**, *9*, 455.
(6) Szabo, A.; Schulten, K.; Schulten, Z. *J. Chem. Phys.* **1980**, *72*, 4350.
(7) Battezzati, M.; Perico, A. *J. Chem. Phys.* **1981**, *74*, 4527.
(8) Battezzati, M.; Perico, A. *J. Chem. Phys.* **1981**, *75*, 886.
(9) Weiss, G. H. *J. Chem. Phys.* **1984**, *80*, 2880.
(10) Pastor, R. W.; Zwanzig, R.; Szabo, A. *J. Chem. Phys.* **1996**, *105*, 3878.
(11) Seki, K.; Barzykin, A. V.; Tachiya, M. *J. Chem. Phys.* **1999**, *110*, 7639.
(12) Srinivas, G.; Sebastian, K. L.; Bagchi, B. *J. Chem. Phys.* **2002**, *116*, 7276.
(13) Jun, S.; Bechhoefer, J.; Ha, B.-Y. *Europhys. Lett.* **2003**, *64*, 420.
(14) Chen, J. Z. Y.; Tsao, H.-K.; Sheng, Y.-J. *Phys. Rev. E* **2005**, *72*, 031804.
(15) Friedman, B.; O'Shaughnessy, B. *Phys. Rev. Lett.* **1988**, *60*, 64.
(16) Friedman, B.; O'Shaughnessy, B. *Phys. Rev. A* **1989**, *40*, 5950.
(17) Yeung, C.; Friedman, B. *J. Chem. Phys.* **2005**, *122*, 214909.
(18) Yeung, C.; Friedman, B. *Europhys. Lett.* **2006**, *73*, 621.
(19) Sung, J.; Lee, J.; Lee, S. *J. Chem. Phys.* **2003**, *118*, 414.
(20) Ortiz-Repiso, M.; Freire, J. J.; Rey, A. *Macromolecules* **1998**, *31*, 8356.
(21) Ortiz-Repiso, M.; Rey, A. *Macromolecules* **1998**, *31*, 8363.
(22) Sheng, Y.-J.; Hsu, P.-H.; Chen, J. Z. Y.; Tsao, H.-K. *Macromolecules* **2004**, *37*, 9257.
(23) Friedman, B.; O'Shaughnessy, B. *Macromolecules* **1993**, *26*, 4888.
(24) Podtelezhnikov, A.; Vologodskii, A. *Macromolecules* **1997**, *30*, 6668.
(25) Zhou, H.-X. *J. Chem. Phys.* **1998**, *108*, 8139.
(26) Klenin, K. V.; Langowski, J. *J. Chem. Phys.* **2004**, *121*, 4951.
(27) Chen, J. Z. Y.; Tsao, H.-K.; Sheng, Y.-J. *Europhys. Lett.* **2004**, *65*, 407.
(28) Newman, M. E. J.; Barkema, G. T. *Monte Carlo Methods in Statistical Physics;* Oxford University Press: New York, 1999.
(29) Binder, K. *Monte Carlo Simulation in Statistical Physics;* Springer-Verlag: New York, 1988.
(30) Carmesin, I.; Kremer, K. *Macromolecules* **1988**, *21*, 2819.
(31) Deutsch, H. P.; Binder, K. *J. Chem. Phys.* **1991**, *94*, 2294.
(32) Le Guillou, J. C.; Zinn-Justin, J. *Phys. Rev. Lett.* **1977**, *39*, 95.
(33) Hahn, T. D.; Kovac, J. *Macromolecules* **1990**, *23*, 5153.